

New Three-Dimensional Bioactive Reinforcing Filler for Improving the Properties of Biomedical Polymers: Synthesis and Application

Mehdi Sadat-Shojai,* Mohammad Kalantari-Lalari, and Milad Asadnia

Cite This: *ACS Omega* 2024, 9, 2192–2203

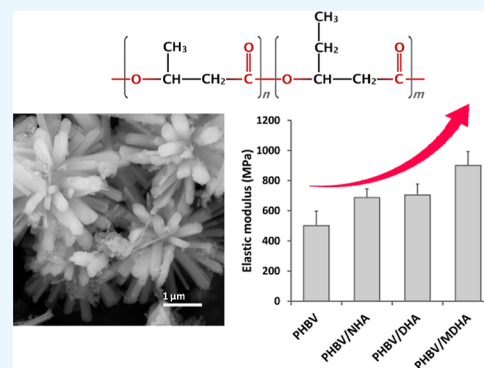
Read Online

ACCESS |

Metrics & More

Article Recommendations

ABSTRACT: In general, the efficiency of reinforcement for filler-based composites is greatly influenced by the filler properties. While much research has been conducted on filler percentage and filler–matrix bonding quality, there is not much research directed to the effect of filler geometry. Therefore, the aim of this article is to examine how a three-dimensional (3D) bioactive filler influences the strength enhancement of biomedical polymers. This was accomplished by first synthesizing highly regular dandelion-like hydroxyapatite (DHA) as a 3D bioactive filler using an optimized hydrothermal method, followed by surface modification with silane molecules. Poly(3-hydroxybutyrate-co-3-hydroxyvalerate) (PHBV) was then used as a biomedical polymer model to fabricate solution-casted composites by using the as-synthesized DHA particles. The results showed that the composites loaded with the surface-modified DHA particles had significantly higher tensile strength and elastic modulus compared to the neat PHBV and composites having irregular particles. In addition to the mechanical properties, our research found that the 3D DHA filler had a significant impact on the biological characteristics of the PHBV, such as water wettability, biodegradability, bioactivity, and in vitro cell response. These findings suggested that particle geometry can play a more significant role in affecting the biological and mechanical performance of biomedical polymers than previously thought.



1. INTRODUCTION

Biomedical polymers have been widely proposed in recent years for a variety of dental and orthopedic applications. However, most biopolymers suffer from undesired compressive modulus and lack the necessary bioactivity. As a result, in academia and industry, the development of composite-based materials containing a polymeric phase and a bioactive ceramic-based filler is regarded as a promising and interesting approach for various biomedical applications. It is expected that the combination of a biopolymer and a bioactive ceramic even at low loading levels will enhance mechanical strength in comparison to the bare polymers and increase ductility and processability in comparison to the brittle ceramics.^{1–3}

In general, filler characteristics such as particle size, geometry, surface area, surface reactivity, volume fraction, degree of particle dispersion and distribution, crystallinity, and the bonding quality between filler and matrix (i.e., filler–matrix adhesion) have a large impact on the efficiency of reinforcement for filler-based composite materials.^{4–6} While many research studies have been conducted on some of these characteristics such as filler percentage and bonding quality,^{5,7} according to the literature, there is not much research directed to the effect of filler geometry. However, compared to the existing fillers with simple geometries like sphere or rod, complicated geometries like three-dimensional (3D) structures may be more prone to increased tensile strength and elastic

modulus of the polymer matrix owing to their complex nature, large surface area, and fewer surface defects.^{8,9} In other words, complicated geometries may have a higher strengthening and toughening impact as a result of enhanced mechanical interlocking, improved crack bridging, and high crack deflection, which can efficiently consume the fracture energy. Moreover, due to the good interfacial interaction and adhesion with the polymer matrix, such geometries can transfer successive loads from the polymer matrix to the rigid particles, hindering the movement and migration of polymer molecular chains. To the best of our knowledge, however, the combination of bioactive fillers with 3D geometries and biomedical polymers has not yet been reported.

In recent decades, various bioactive ceramic-based fillers, the most well known of which is hydroxyapatite (HA), have been used in combination with biomedical polymers. HA with chemical formula of $\text{Ca}_{10}(\text{PO}_4)_6(\text{OH})_2$ has some outstanding properties such as bioactivity, biocompatibility, low cytotoxic

Received: July 24, 2023

Revised: December 15, 2023

Accepted: December 22, 2023

Published: January 2, 2024



icity, affinity to biopolymers, identical chemical composition with natural bones, high osteoconduction and osteointegration potential, ability to replace toxic ions, and low water solubility.¹⁰ Because of its remarkable stiffness, the HA filler can increase the elastic modulus and compressive strength of the polymer matrix.^{11,12} HA particles with one- and two-dimensional (1D and 2D) geometries have been synthesized using different processes such as hydrothermal synthesis,¹³ precipitation,¹⁴ hydrolysis,¹⁵ solid state synthesis,¹⁶ and sol-gel crystallization.¹⁷ In comparison to the 1D and 2D geometries, little effort has been made to synthesize the 3D geometry of HA, which is due to the complicated procedure, which results in nonuniformity of the synthesized particles in terms of size and, as a result, their inapplicability as biomedical fillers. Accordingly, the reinforcing effect of 1D and 2D HA on various biomedical polymers has been investigated, but to the best of our knowledge, no study on the fabrication of polymer matrix with 3D HA reinforcement exists.

Because of their excellent physical and chemical properties, poly(hydroxyalkanoates) (PHAs) are a popular biomedical polymer in science and industry. PHAs are a type of biocompatible polyester that is produced by fermenting alkanes, alkenes, sugars, lipids, and alkanolic acids with various Gramme positive and Gramme negative bacteria.^{18–20} More than 90 different types of PHAs composed of various monomers are known, and the number is growing. The first PHA discovered by the French bacteriologist Maurice Lemoigne in 1926 was poly(3-hydroxybutyric acid) (PHB).^{21,22} For decades, PHB has been studied as the most common and basic member of the PHA family. PHB, on the other hand, has poor processability and is brittle, limiting its potential applications.²³ Therefore, many researchers have developed PHB copolymers, such as poly(3-hydroxybutyrate-co-3-hydroxyvalerate) (PHBV), to address these limitations. However, like the other organic polymers, PHBV lacks the desired compressive modulus and bioactivity. Therefore, the use of ceramic-based fillers such as HA is vital to improve these undesirable characteristics. For example, Öner and İlhan²⁴ as well as Degli Esposti et al.²⁵ reported that mechanical properties of biodegradable PHBV can be significantly improved by embedding the HA having spherical geometry in the polymeric matrix. In our recent study,²⁶ we used HA with rod-like geometry in combination with PHBV (up to 15%) which, according to the results, increased the tensile strength and elastic modulus of the composite up to 85 and 110%, respectively. Therefore, it will be interesting to evaluate the hypothesis that the use of HA filler with a more complicated geometry (i.e., 3D morphology) can additionally increase the mechanical characteristics of the PHBV biopolymer.

This article is a follow up to our previous studies^{26–28} on PHA/HA composites and especially aims at investigating the effect of a 3D bioactive filler on the strength enhancement of biodegradable polymers. For this purpose, highly regular dandelion-like HA (DHA) as a 3D bioactive filler was first synthesized through an optimized hydrothermal method. PHBV was then used as a biomedical polymer model to fabricate solution-casted composites using the as-synthesized DHA particles. Several control groups were employed to determine the effect of the filler–matrix interface, geometry, and filler percentage on mechanical and biological properties. Furthermore, we investigated the effect of the 3D bioactive

filler on the in vitro cell response of the newly fabricated constructs.

2. EXPERIMENTAL SECTION

2.1. Synthesis of DHA Particles. 3D DHA particles were synthesized in-house using a hydrothermal method. For this, 8.83 g of ethylenediaminetetraacetic acid disodium salt dihydrate ($\text{Na}_2\text{EDTA}\cdot 2\text{H}_2\text{O}$, Merck) and 7.5 mL of urea (Merck) solution of 0.2 M concentration, together with 5.9 g of $\text{Ca}(\text{NO}_3)_2\cdot 4\text{H}_2\text{O}$ (Merck), were dissolved in 25 mL of deionized water and agitated for 30 min to make a uniform solution. Under constant and mild stirring, 0.06 M phosphate ion solution (made from $(\text{NH}_4)_2\text{HPO}_4$, Merck) was dropped into the Ca/EDTA/urea solution, while Ca/P remained at its stoichiometric value in HA (1.67). To control the pH to 7, an NH_4OH solution (Merck) was added to the mixture, which was then stirred for 20 min. A cylindrical stainless steel autoclave with a Teflon coating was then used to treat the HA precursor hydrothermally at 200 °C for 18 h. The powder obtained was finally washed four times with a 25:75 mixture of deionized water and ethanol, centrifuged, dried for 6 h at 60 °C, and then crushed.

The phase composition and chemical groups of the powder were determined using the X-ray diffraction (XRD) method and Fourier-transform infrared (FTIR) spectroscopy, respectively. Furthermore, by using the XRD pattern, the degree of crystallinity (X_c), crystallite size (D), and crystalline phase of particles were evaluated following the methods documented in the literature.^{13,29} The Ca/P ratio of the powder was examined by inductively coupled plasma optical emission spectrometry (ICP-OES; Model Vista-Pro, Varian). For this, the sample was dissolved in 0.1 mol/dm³ nitric acid (Merck), and ICP calibration curves were prepared using standard reference materials. The morphology, particle size, and particle size distribution of the powder were investigated by using scanning electron microscopy (SEM, Vega3, TESCAN, Czech Republic) and transmission electron microscopy (TEM, CM10, Philips, Netherlands). The specific surface area of the particles was determined using the Brunauer–Emmett–Teller (BET) method using a nitrogen absorption isotherm apparatus (Costech Instruments, Sorptometer Kelvin 1042). To assess the bioactivity of the synthesized particles, a simulated body fluid (SBF) solution with ion concentrations comparable to those of blood plasma was used. For this, SBF solution was prepared according to a previously reported protocol,³⁰ and the powder was soaked in the solution for 15 days at 37 °C. The SBF solution was also renewed every 3 days to further simulate physiological conditions. The powder sample was analyzed with SEM after filtration and washing with deionized water.

2.2. Surface Modification of DHA Particles. DHA particles were surface-modified using trimethoxy(propyl)silane (TMPS) (Sigma-Aldrich). For this, the particles (100 mg) were kept in a vacuum chamber at 60 °C for 24 h before being ultrasonically dispersed in 5.0 mL of anhydrous toluene (Merck) for 30 min. The resultant solution/dispersion was refluxed at 110 °C for 24 h while being vigorously stirred after the addition of TMPS (4.0 mL). Following the grafting procedure, the modified DHA (dubbed MDHA) was separated from the dispersing solvent by centrifugation at 3900 rpm for 10 min, thoroughly rinsed with ether to remove the physically attached silane molecules, and dried at 60 °C for 16 h. To chemically confirm the surface modification, we carried out

FTIR analysis. Moreover, grafting density of TMPS to particles was determined according to the method described in the literature.³¹ The colloidal stability of unmodified and surface modified particles was also investigated by using sedimentation experiments. The powder was dispersed in chloroform (Fluka) at a particle loading of 1 mg/mL using a water bath sonicator, and the suspensions were allowed to stand for 48 h, while the particle sedimentation behavior was recorded at various time intervals.

2.3. Fabrication of PHBV/DHA Composites. PHBV (Sigma-Aldrich) with 5% 3-hydroxyvalerate (HV) content and an average molecular weight of 2.9×10^5 g/mol (determined by viscometry) was used in the current study. Moreover, we used natural bovine HA (NHA, prepared from Amirkabir University of Technology) as control filler. Figure 1 shows

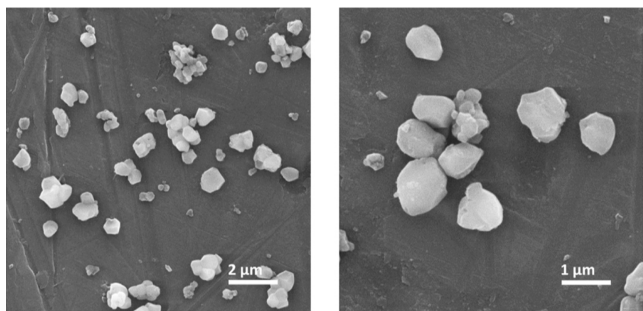


Figure 1. SEM spectral micrographs of NHA at different magnifications

SEM of NHA at different magnifications, indicating an irregular geometry with an average particle size of around 0.5 μm . To increase filler dispersion in the polymer matrix, we combined a solution casting method with an ultrasonic device. In brief, to fabricate PHBV composites with 15 wt % filler content with respect to the polymer (higher filler content may cause agglomeration), an ultrasonic bath was first used for a full dispersion of filler (26 mg) in dry chloroform (5 mL) for 5 min at room temperature. After addition of 175 mg PHBV under a concentration of 3.5 wt % (this polymer concentration was optimized based on the colloidal stability of the particles in the final solution), the solution was stirred and refluxed at 65 $^{\circ}\text{C}$ for 6 h, followed by 5 min of further sonication. The solution/dispersion was poured into a glass mold (Petri dish), covered, and kept in the fume hood until the solvent had completely evaporated. The resulting dried films were then vacuum-dried for 48 h to remove any remaining chloroform solvent. Three control groups were used to investigate the effects of various parameters on the characteristics of the as-fabricated composites: (1) a bare PHBV film without any particles, used to assess the impact of filler loading, (2) a PHBV composite film incorporated with NHA, used to determine the impact of filler geometry, and (3) a PHBV composite film incorporated with ungrafted DHA structures, used to evaluate the impact of TMPS-grafting to the DHA particles.

SEM was used to examine the morphology of the fabricated composites, while an energy dispersive X-ray spectrometer (EDX, QX2, Rontec) was used to evaluate the dispersion of the HA filler inside the film. The influence of the filler type on the crystallization of PHBV biopolymer was studied using differential scanning calorimetry (DSC, Model 200-F3, Netzsch, Germany) in a flowing N_2 atmosphere. For this, at

a heating rate of 50 $^{\circ}\text{C}/\text{min}$, the polymer sample was heated to 190 $^{\circ}\text{C}$ and held for 2 min in order to eliminate any potential nuclei that could serve as seed crystals. The sample was then cooled to -20 $^{\circ}\text{C}$ at a cooling rate of 10 $^{\circ}\text{C}/\text{min}$ and then reheated to 190 $^{\circ}\text{C}$ at the same rate of 10 $^{\circ}\text{C}/\text{min}$ to record the endothermic melting peak. The mechanical properties of the prepared film were evaluated using rectangular specimens prepared by cutting the films at dimensions of ~ 0.1 mm \times 5 mm \times 10 mm. A universal testing device (Z020, Zwick/Roell, Germany) with a 20 N load cell was used for the experiments. The crosshead moved at a constant rate of 0.5 mm/min at a temperature of 25 ± 2 $^{\circ}\text{C}$. The maximum strength derived from the stress–strain curves was then considered as the tensile strength. The tensile modulus was also determined using the slope of the curve's initial linear area. For each sample group, five measurements were taken, and the results were reported as the mean \pm standard deviation (SD). To estimate the change in hydrophilicity/hydrophobicity of composite films with the type of filler, water contact angles of films were measured using a Dino-Lite Premier contact angle camera (AM-7013MZT), and the contact angle was analyzed by SCA20 (Dataphysics) software. For each sample, 1.0 μL of deionized water was placed on the surface and an instantaneous image of the water droplet was taken. The contact angle was then determined from this image and presented as the mean \pm SD of the three measurements. To assess the in vitro biodegradation, composite samples were cut into 10 \times 10 mm square pieces in triplicate, weighed, and immersed in 15.0 mL of 1 \times phosphate-buffered saline (PBS, Invitrogen) at 37 $^{\circ}\text{C}$, and the weight loss was then measured every 7 days for the predicted time (6 weeks). For in vitro bioactivity analysis, the composite samples were immersed in SBF solution for 30 days at 37 $^{\circ}\text{C}$ in an incubator, with the SBF solution being renewed every 3 days. The samples were taken from the solution, rinsed with deionized water, and completely dried before being analyzed by SEM.

2.4. In Vitro Cell Assays. The mouse calvarial preosteoblastic cell line (MC3T3-E1) was used in the current study for in vitro cell experiments, and Minimum Essential Medium Alpha Medium (α -MEM, Invitrogen) was used as the culture medium. α -MEM was mixed with 1% penicillin–streptomycin (Invitrogen) and 10% fetal bovine serum (FBS, HyClone). It was used to determine the biocompatibility of the as-synthesized DHA powder. For this, MC3T3-E1 cells at 70% confluence were washed using PBS, detached by applying trypsin (Sigma-Aldrich), and then suspended in the fresh α -MEM. The resulting cells were subsequently seeded into the 24-well plates at the concentration of 4×10^3 cells per well and incubated in α -MEM in the incubator at 37 $^{\circ}\text{C}$. After 1 day, DHA particles suspended in α -MEM at a concentration of 0.1 mg/mL were added to the culture wells, and the cultures were incubated for 3 days. Finally, the viability of MC3T3-E1 cells cultured with DHA particles was assessed using the calcein-AM/ethidium homodimer-1 (EthD-1) Live/Dead kit (Invitrogen) as directed by the manufacturer. A fluorescence microscope (Leica Microsystems; Germany) was used to capture the images of alive and dead cells, and the number of living and dead cells was calculated using ImageJ software. In order to evaluate the interaction of the bone cells with the fabricated composites, defect-free PHBV/MDHA films were sterilized in 70% ethanol for 2 h before being washed in autoclaved deionized water. 30 μL of a concentrated cell suspension containing 8×10^3 cells was applied to the films,

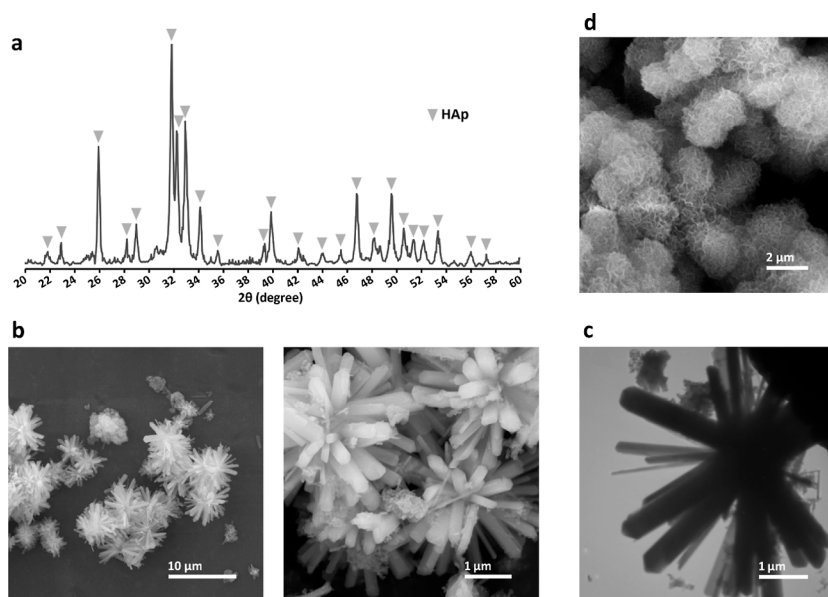


Figure 2. Characterizations of DHA particles: (a) XRD pattern; (b) SEM photomicrographs at different magnifications; (c) TEM photomicrograph; and (d) SEM photomicrograph after 15 days of incubation of particles in SBF under physiological conditions

and the cells were allowed to adhere to the surface of the samples. After this step, α -MEM was added, and samples were maintained in the incubator for the time periods specified, while the culture medium was refreshed every 2 days and the PHBV film without filler was served as control. In this study, metabolic activity of the cultured bone cells at days 1, 4, and 7 was evaluated by the Alamar Blue (AB, Invitrogen) method. In summary, following the removal of the medium from the culture wells, the AB solution was diluted with α -MEM at a ratio of 1:10 and subsequently applied directly to the samples. The samples were then incubated at 37 °C for 3 h. After the AB solution was transferred to 96-well plates, the chemical reduction induced by bone cell metabolism was measured using a microplate reader with an excitation at 544 nm and emission at 590 nm. The percent reduction of Alamar Blue was then determined according to the vendor's instructions. To measure cell proliferation on the PHBV/MDHA composite, DNA was quantified using the PicoGreen (Invitrogen) test. For this purpose, after cell seeding, each sample was transferred to an Eppendorf tube filled with 500 mL of ultrapure water followed by a 10 min vigorous vortexing. An equal volume of PicoGreen reagent diluted 200-fold in 1 \times TE buffer (Invitrogen) was added to the mixture of each sample and 1 \times TE buffer, followed by a reading of the fluorescence intensity at 485 nm excitation/520 nm emission. Based on manufacturer's instructions, the reading values were converted to DNA concentrations in μ g/mL using a standard calibration curve built using a range of known concentrations of double-stranded DNA (dsDNA) solutions. A total of six measurements were conducted for each sample group in both the AB and DNA analyses, and the resulting values were reported as mean \pm SD. To stain nuclei, MC3T3-E1 cells were first fixed with 4% paraformaldehyde in PBS for 15 min, followed by addition of a solution of 4',6-diamidino-2-phenylindole (DAPI, Invitrogen) in PBS with a concentration of 1 μ L/mL. Following a 5 min incubation period at 37 °C, the samples were subjected to a rinse with PBS and subsequently stored in a light-restricted environment until they were examined using fluorescence microscopy. Calcium deposition on composite

films was investigated using Alizarin Red-S (Sigma) staining in which calcium forms a complex with Alizarin Red in a chelating process. At 7 and 14 days, after the initial MC3T3-E1 cell seeding, the samples were fixed with 4% paraformaldehyde in PBS, washed twice with deionized water, and incubated for 20 min at room temperature with a freshly produced 2% Alizarin Red solution (pH 4.2) in water. The samples were subsequently washed thoroughly with deionized water, and the stained samples were then photographed using a digital camera. To quantitatively evaluate the differentiation of MC3T3-E1 cells, the matrix mineralization was quantified by the extraction of the minerals at low pH following the protocol described elsewhere.⁵

2.5. Statistics. We compared quantitative data using Tukey's test and one-way analysis of variance (one-way ANOVA). In this study, *p*-values less than 0.05 were considered statistically significant.

3. RESULTS AND DISCUSSION

3.1. Characterization of DHA Particles. The current study used XRD, ICP-OES, SEM, and TEM to characterize 3D DHA particles. Moreover, both the bioactivity and in vitro cell biocompatibility of DHA particles were also investigated. According to the XRD pattern (Figure 2a) and the ICDD card no. 09-0432, the DHA particles were of pure HA. The XRD results indicate 95 nm for *D* (for an isolated peak assigned to 0 0 2 plane) and 88% for *X_c*. According to the ICP-OES measurement, the Ca/P ratio of DHA was 1.69, which is remarkably close to the stoichiometric ratio of 1.67. Based on the SEM and TEM micrographs (Figure 2b,c), the as-synthesized DHA particles show an intriguing dandelion-like shape with hexagonal nanorods converging to a single center. The overall size of these assembled structures is roughly 5 μ m, and the diameters of the nanorods range from 300 to 500 nm. On the other hand, from the BET results, the specific surface area was 62 m²/g. It was hypothesized that these DHA particles could improve the mechanical properties and, to a lesser extent, the biological properties of polymer-based

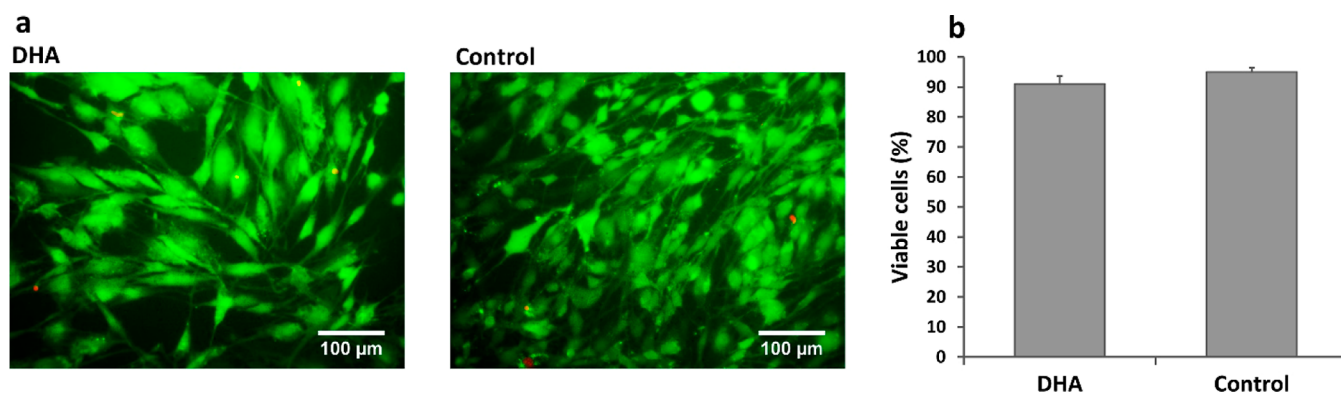


Figure 3. (a) Representative micrographs of live/dead staining (a) and related quantification of viable cells (b) of MC3T3-E1 preosteoblast cells cultured in the presence of DHA particles in comparison with the control (tissue culture plastic surface)

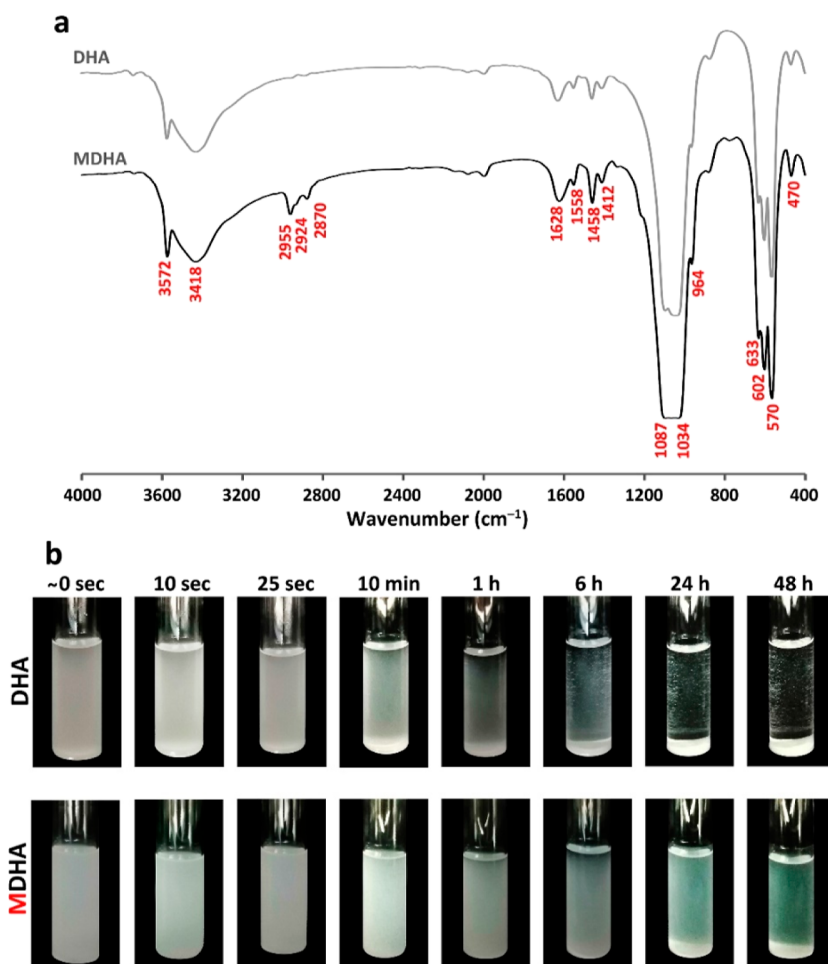


Figure 4. (a) FTIR spectra of unmodified and modified DHA particles and (b) colloidal stability of MDHA particles dispersed in chloroform in comparison with the control (i.e., unmodified DHA) during different time intervals

composites due to their complex shape, small particle size, and notable specific surface area.

The *in vitro* assessment of mineralization on a particular surface can be accomplished through the utilization of a conventional technique involving SBF solution, which was initially proposed by Kokubo and Takadama.³⁰ Our findings show that after 15 days of incubation in SBF, DHA can undergo a morphological change from dandelion-like to flake-like shape, as shown in the SEM micrographs in Figure 2d. The observed phenomenon can be attributed to the concurrent

dissolution–recrystallization mechanism, which results in the formation of a new apatite phase during the incubation of the powder in SBF. It is also expected that the same thing will happen *in vivo*, that is, after implanting HA particles, either as a pure ceramic or as a composite, a new apatite appearance should grow on the surface of HA crystals. These findings indicate that the synthesized powder has a high level of bioactivity, indicating its potential use in bone regeneration applications.

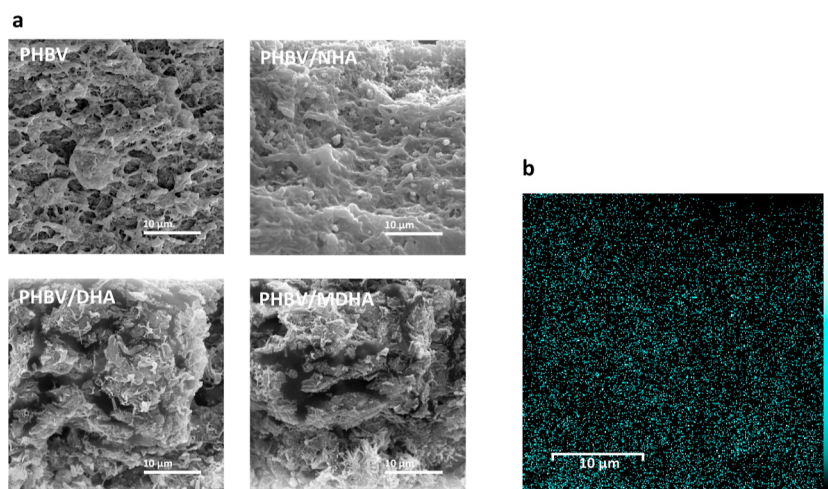


Figure 5. (a) Representative cross-sectional SEM photomicrograph of the as-fabricated composite films containing NHA, DHA, and MDHA in comparison with the control (i.e., neat PHBV); (b) cross-sectional EDX-mapping of filler particles embedded in the MDHA/PHBV film

The suitability of the DHA particles synthesized in this study for use in bone tissue engineering applications was also validated by assessing the viability of preosteoblast cells (MC3T3-E1) when exposed to the particles at 0.1 mg/mL concentration. This concentration was chosen because a significant change in the ionic concentrations (calcium and phosphate levels) of the culture medium can occur at higher concentrations. Figure 3a,b shows the fluorescence images and related quantification of the living cells after 3 days of culture, respectively. According to the findings, there was no discernible difference in cell viability between the control group (cells cultured on a tissue culture plastic surface) and DHA particles after 3 days of incubation, indicating that the synthesized DHA powder is highly biocompatible. In other words, the DHA particles generated here have a high potential for use in close contact with bone cells.

3.2. Characterization of Surface-Modified DHA. Surface modification of reinforcing mineral fillers is an important step in the fabrication of polymer composites.^{32–34} Therefore, the DHA particles synthesized here were treated with the TMPS reagent. According to the hypothesized mechanism, the oxygen atom of the hydroxyl group on the surface of DHA particles is initially activated by creating hydrogen bonds, which is subsequently followed by a nucleophilic attack on the silicon. Finally, surface modification is accomplished through the liberation of methanol molecules. Based on this mechanism, the strong affinity between oxygen and silicon is critical to the treatment's efficacy.³⁴ The modification of DHA particles with TMPS molecules was confirmed by FTIR (Figure 4a). According to the results, while FTIR absorption bands corresponding to OH⁻ groups in adsorbed water (3418 and 1628 cm⁻¹), crystalline OH⁻ (3572 and 632 cm⁻¹), and PO₄³⁻ groups (1087, 1034, 964, 602, 570, and 470 cm⁻¹) were detected for the HA structure in FTIR spectrum, the bonding of silane reagent with DHA was demonstrated by the symmetric/asymmetric stretches of methylene and methyl groups in the silane molecules at 2870, 2924, and 2955 cm⁻¹. From Figure 4a, it can also be seen that there are weak peaks at 1400–1600 cm⁻¹ (1558, 1458, and 1412 cm⁻¹) which should be attributed to the carbonate absorption band, indicating the presence of low amounts of carbonate impurities in the crystal structure of DHA particles. According to our results, the grafting density of silane was found to be 2.44 molecule/nm².

The colloidal stability analysis was used to confirm the particle surface modification. The sedimentation test findings of DHA and modified DHA suspended in chloroform are shown in Figure 4b. Based on the data presented in the figure, the aggregation and subsequent precipitation of the unmodified DHA particles began shortly after the sonication process. The suspensions had separated into sediments with a clear supernatant on top after 1 h. On the other hand, during 2 days of monitoring, the sedimentation behavior of DHA particles modified with TMPS was seen in the form of cloudy suspensions, demonstrating a significantly higher colloidal stability. These findings imply that modified particles will remain stable in the organic phase during the solution casting process, which is critical for preventing filler agglomeration and aggregation in the final composites. The results are consistent with our previous findings,²⁶ which show that surface modification of HA powder by silane molecules could successfully avoid powder aggregation and greatly improve the powder interfacial interaction with the polymer matrix.

3.3. PHBV/DHA Composites. In this study, we first synthesized a 3D DHA filler with unique properties and then fabricated PHBV/DHA composites with 15% filler content (with respect to the polymer) using the solution casting method to test the hypothesis that this 3D filler can significantly improve the mechanical properties of biomedical polymers compared to traditional fillers. Here, the time of solvent evaporation during the solution casting process was optimized to 3 h to reduce filler sedimentation as much as possible. The viscosity of the polymer solution is another important parameter in the solution casting method. If the viscosity is high, then the resistance to sedimentation will also be high. Therefore, increasing the viscosity will increase the dispersity of fillers in the bulk of composites. In this study, the polymer concentration (3.5 wt %) and the concentration of particles (15 wt %) in the solution were optimized for all composites based on the colloidal stability and viscosity of particles in the final solution/dispersion.

The morphology and homogeneity of composites, particularly the homogeneous dispersion and distribution of filler throughout the polymer matrix, are important parameters because they strongly affect the final properties and performance of composites.^{35,36} Figure 5a shows cross-sectional SEM micrographs of the fabricated composites. According to the

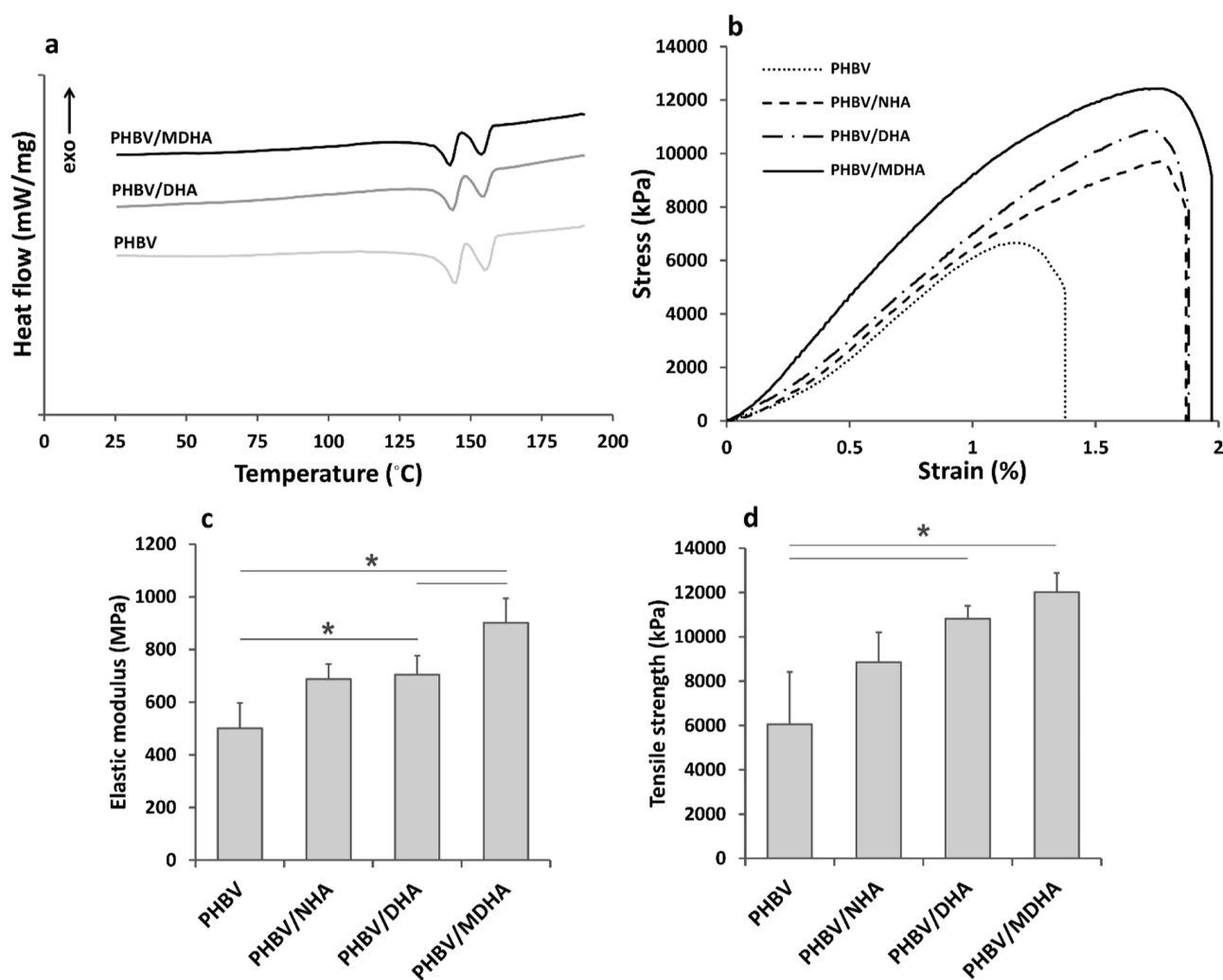


Figure 6. Thermal and mechanical characterization of as-fabricated composites: (a) DSC curves of the composites containing DHA and MDHA in comparison with the control (i.e., neat PHBV); (b) representative stress–strain curves obtained for the PHBV/DHA and PHBV/MDHA and controls, i.e., PHBV/NHA and neat PHBV; elastic modulus (c) and tensile strength (d) of the composites and controls determined from the stress–strain curves; all data are mean \pm SD of five measurements, and the inserted asterisk (*) denotes a statistically significant difference ($p < 0.05$) between the experimental groups.

results, a rougher cross section was identified for the PHBV/DHA composites compared to the neat polymer (i.e., PHBV) and the PHBV/NHA composite. Furthermore, when surface-modified DHA particles were incorporated into the PHBV (i.e., PHBV/MDHA), an additional rougher cross section was detected when compared to that of the controls. Accordingly, the cross-sectional pattern of the film changes in the presence of HA filler with different characteristics. A more uneven cross section may indicate greater mechanical strength, a feature that requires more examination by using mechanical analysis. In addition to geometry, the dispersion of fillers in the polymer matrix is an important factor in the fabrication of filler-based composites with enhanced mechanical and homogeneous bulk properties. To obtain more evidence for the dispersion/distribution of the MDHA particles within the PHBV matrix, the PHBV/MDHA composite cross section was investigated using EDX-mapping of Ca ions (Figure 5b). According to the EDX-mapping analysis, the uniform dispersion and distribution of surface-grafted DHA in the polymer model were clearly validated. When modified DHA (i.e., MDHA) is combined with a polymer in a solution, the increased particle–polymer interaction improves the interfacial adhesion between the two

phases, resulting in uniform dispersion of MDHA in the polymer matrix.

In contrast to amorphous materials, crystallizable polymers, such as PHBV, crystallize as spherulites from the melt; thus, to investigate the effect of filler content on polymer crystallinity, the thermal behavior of the neat polymer and composites containing DHA and MDHA particles was examined using DSC, as shown in Figure 6a. The DSC curves show that all the three samples have two melting endothermic peaks, and the temperature of both the peaks for the composite samples (PHBV/DHA and PHBV/MDHA) is slightly lower than that for the neat polymer (PHBV). The melting temperature of the polymer composites is affected by a number of factors, including morphology, crystallization ability, and composition.³⁷ The slight decrease in the melting temperature of the polymer in the presence of either DHA or MDHA can be attributed to the hindrance of the 3D filler particles to bring the polymer chains closer together.

The effects of the incorporation of HA filler with the dandelion geometry on the mechanical properties of the PHBV matrix as a biomedical polymer model were investigated by tensile testing. The typical stress–strain curves obtained for

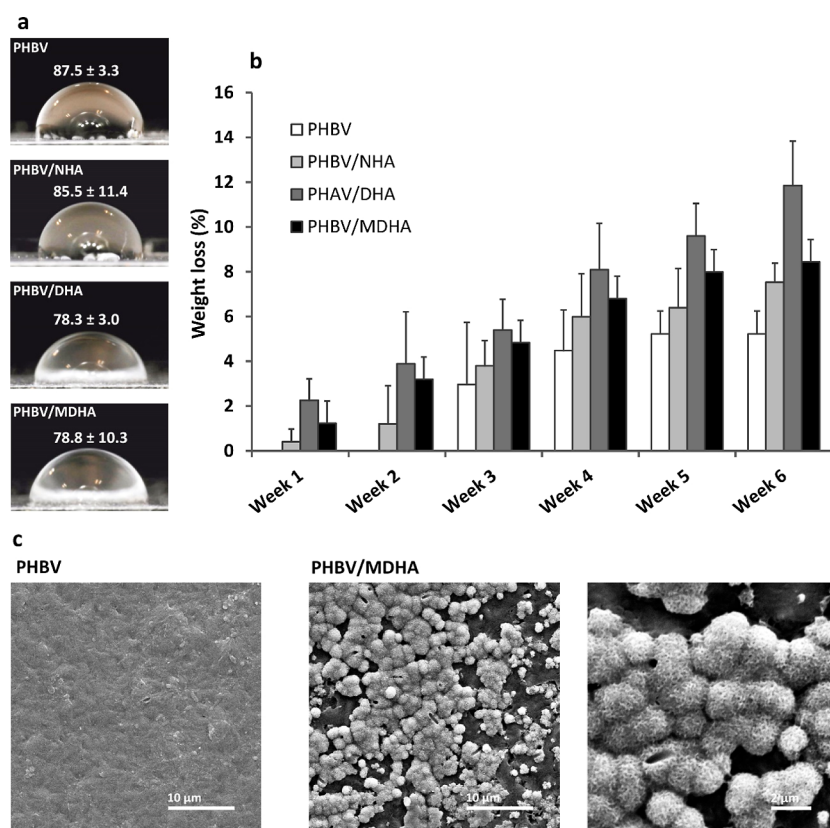


Figure 7. Representative images of the wettability estimation (a) and biodegradability (b) for PHBV/DHA and PHBV/MDHA and controls, i.e., PHBV/NHA and neat PHBV; the measurement of mass loss in the biodegradability test was performed in PBS at 37 °C, and the results are the mean \pm SD of three measurements; (c) representative SEM photomicrographs of the MDHA/PHBV composite at two different magnifications in comparison with neat PHBV after 15 days of incubation in SBF at 37 °C

fabricated composites and controls are shown in Figure 6b. According to the figure, the bare PHBV film had a linear elastic zone at first, followed by a breaking point. The addition of NHA, DHA, and MDHA significantly increased the maximum tension of the films, as well as the slope of the curves. Based on the stress–strain curves, the Young’s modulus and tensile strength of the films were determined, as depicted in Figure 6c,d, respectively. Here, based on the findings, the hypothesis that we proposed at the beginning of the article was confirmed, so that the composite with 3D filler (DHA and MDHA) had a surprisingly higher tensile strength and elastic modulus than the pure polymer, as well as the composite with irregular filler (i.e., NHA). Moreover, the PHBV/MDHA film had the highest tensile strength ($12,020 \pm 870$ MPa) and tensile modulus (902 ± 93 MPa), indicating the synergistic effects of geometry and filler surface properties on mechanical properties of the final composite. The SEM images in Figure 5a also show a much rougher cross section for the DHA-based composites when compared to the NHA-based composites and neat polymer, indicating a significant change in mechanical strength. The use of reinforcing fillers with a complex geometry such as DHA in polymer matrices results in a rougher cross-sectional area during final failure. The reason for this is to prevent the growth of microcracks due to contact with the reinforcement and their constant redirection. In other words, the microcracks collide with each other over short distances, resulting in a very rough surface. Zhao et al. stated that an increase in surface roughness could be used as an evidence for fracture deflection, which increases crack length and, thus, the energy absorbed

during deformation.³⁸ The strength of the polymer composites is significantly influenced by the interfacial bonding between the filler particles and the polymer chains, and as expected, the composite containing the TMPS-grafted filler (i.e., PHBV/MDHA) had significantly higher mechanical strength than the composite incorporated with the bare filler (i.e., PHBV/DHA) (Figure 6c,d). When a high modulus filler with a good interfacial interaction is combined with a lower modulus polymer, it can become closely linked with the polymer chains, making the composite films more difficult to deform under the same load. Furthermore, stress is transferred at the matrix/filler interface via shear and tensile stress, and the rate of load transfer is dependent on the shear and tensile stress. This highlights how the interface affects the polymer modulus. As a result, as the interface improves, the filler’s ability to carry the load improves, resulting in a higher modulus.

To evaluate the biological performance of the as-fabricated composites, contact angle measurements were used to examine their degree of hydrophilicity/hydrophobicity. The contact angle, in turn, is influenced by a variety of factors, including the hydrophobicity of the composite and the surface roughness.³⁹ According to the results (Figure 7a), HA-containing composites in comparison with neat PHBV had a lower water contact angle due to the presence of HA filler as hydrophilic particles. However, the results revealed that the NHA was able to reduce the water contact angle from $87.5 \pm 3.3^\circ$ to $85.5 \pm 11.4^\circ$, which was insignificant, while the DHA significantly reduced the water contact angle to $78.3 \pm 3.0^\circ$. Reduced contact angle increases hydrophilicity, which directly

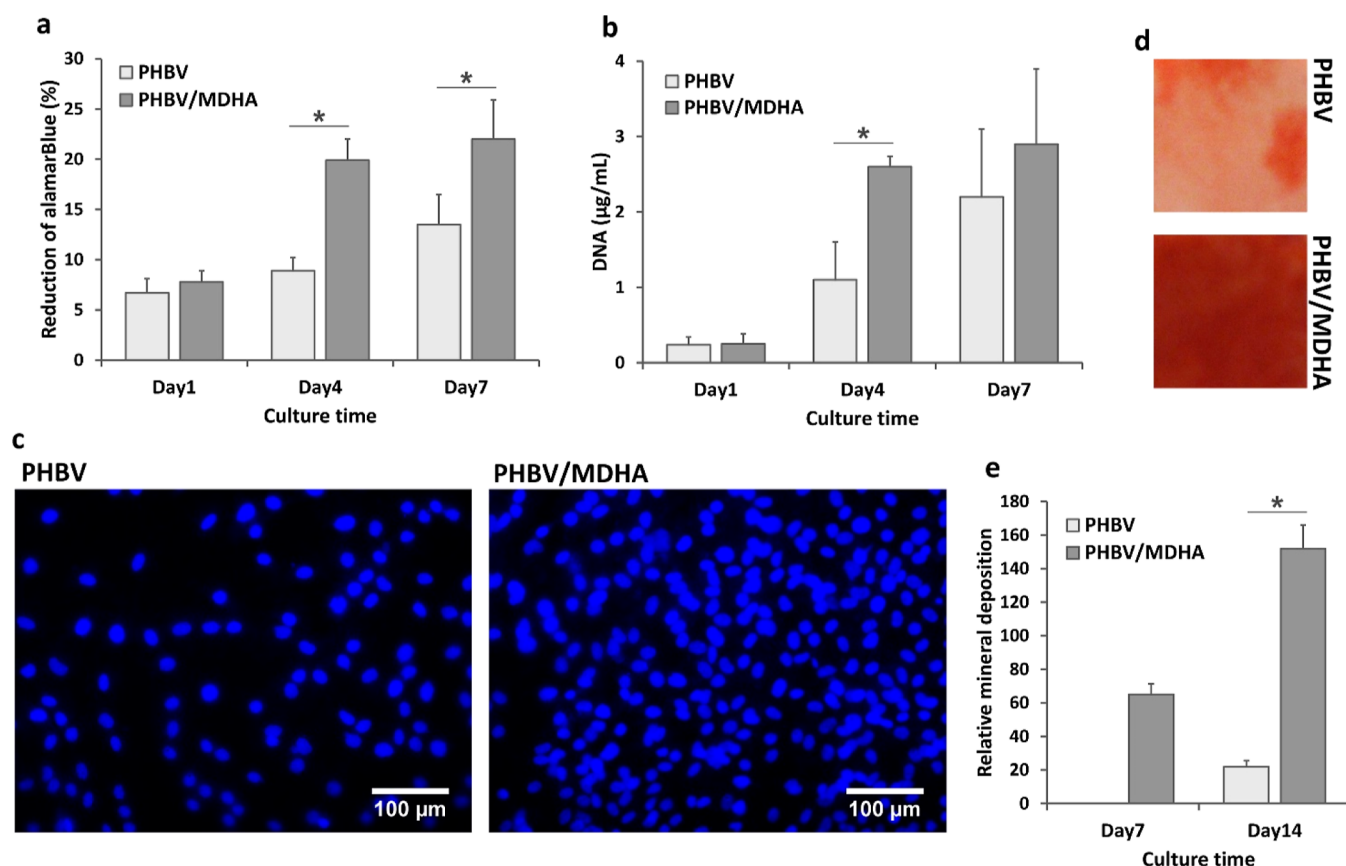


Figure 8. In vitro cell characterization of the MDHA/PHBV composite: metabolic activity (a) and proliferation (b) of MC3T3-E1 preosteoblasts cultured on the surface of the MDHA/PHBV composite in comparison with neat PHBV. (c) Representative fluorescent imaging of MC3T3-E1 preosteoblasts cultured on the surface of the MDHA/PHBV composite and neat PHBV at day 4 of culture. Photographic images of Alizarin Red-S staining for mineralization on the MDHA/PHBV composite in comparison with neat PHBV (d) and the corresponding quantification of minerals that originated from MC3T3-E1 osteogenic differentiation (e); results are the mean \pm SD of six measurements, and asterisks (*) denotes a statistically significant difference ($p < 0.05$) between the experimental groups.

increases the water uptake and, as a result, biodegradability and cell adhesion. On the other hand, according to the results, the water contact angle does not significantly change after the silanization ($78.3 \pm 3^\circ$ for PHBV/DHA compared to $78.8 \pm 10.3^\circ$ for PHBV/MDHA), indicating that surface hydrophilicity cannot be significantly influenced by the surface modification of particles.

In order to allow for the regeneration of totally autologous bone tissues, the implanted scaffold must degrade at the appropriate rate during neo-tissue creation.⁴⁰ In the current study, the weight loss rate of composites was obtained to evaluate the influence of the reinforcing agent on the biodegradability of the PHBV polymer. Figure 7b shows the mass change for the neat PHBV film as well as composites containing 15% NHA, DHA, and MDHA particles incubated in PBS at 37 °C. According to the results, neat PHBV polymer films did not show any biodegradability or weight loss until the end of the second week. PHBV is a crystalline and hydrophobic material that does not allow for considerable water penetration for hydrolysis of ester bonds; thus, in the absence of enzyme and in physiological pH, PHBV is hardly degradable. However, the measurements of weight loss revealed that the PHBV composite incorporated with 15% filler, regardless of the filler type, had a significantly higher weight loss, probably because of an increased water uptake caused by the presence of hydrophilic particles and, as a result,

increased hydrolytic attack on the polymer matrix. Although biodegradability for neat PHBV began in the third week, HA-containing composites still demonstrated a higher degradation rate than the neat polymer. Furthermore, when compared to the composite loaded with NHA, the composite containing DHA had a higher biodegradation rate, which could be attributed to the composite's higher water uptake. Surface-modified DHA, on the other hand, showed less weight loss than untreated DHA, especially in the fifth and sixth weeks. This could be due to the improved mechanical integrity of PHBV/MDHA, which may reduce the water uptake during the degradation study and thus change the rate of degradation.

The PHBV/MDHA composites created here were claimed to be effective for bone healing applications, and therefore, their bioactivity needs to be evaluated. SBF was used as a calcification medium in our study to investigate biomimetic calcification under normal physiological settings. Figure 7c depicts the surface morphology of the PHBV/MDHA composite in comparison to the control (i.e., neat PHBV) after 15 days of incubation in SBF. The figure shows that while a relatively dense apatite layer formed on the surface of the MDHA-filled composite, no apatite growth was observed in the neat polymer. The results also show that new bone nodules generated on the surface of the filled composite had a consistent flake-like shape under high magnification. The high in vitro bioactivity of filled composites compared to the neat

polymer was attributed to the presence of bioactive DHA filler, which led to an enrichment of Ca^{2+} in the SBF solution, resulting in local supersaturation and crystal nucleation.

Although it is generally known that HA ceramics can increase cell proliferation *in vitro*,^{5,41} nothing is known about the effect of 3D HA incorporated in PHBV composites on cellular response. In this study, *in vitro* cell culture was used to assess the feasibility of the fabricated PHBV/MDHA constructs for prospective bone tissue applications. Figure 8a,b shows proliferative activity and DNA quantification of the preosteoblasts cultured on the PHBV/MDHA composites compared with the neat PHBV at the same time points, respectively. Figure 8a clearly illustrates that after 4 and 7 days of culture, the filled sample had more metabolic activity than the control (neat polymer). In particular, the % AB reduction of the PHBV/MDHA composite was >2-fold higher than the neat PHBV on day 4 of culture ($p < 0.05$). The same enhancement, although to a lesser extent, was observed on day 7 when cells approached confluence. Similar to the AB results, the cells cultured on the DHA-filled composites had higher DNA content and therefore were more prone to proliferation compared to the cells cultured on the neat polymer (Figure 8b). Furthermore, the DNA content increased significantly throughout the culture period, indicating that the cells in all groups were alive and growing continuously. Figure 8c depicts the staining of the cell nucleus with DAPI, which was conducted 4 days after the initial cell seeding to visually examine the density of cell attachment. An evident difference could be found between the PHBV/MDHA composite and neat PHBV, consistent with the cell numbers, as reported in Figure 8b. Preosteoblasts can be differentiated into premature osteoblasts and then mature osteoblasts in response to certain stimuli. This process, which is characterized by the production of mineralized nodules, reveals the material's property to induce bone formation.⁵ In this study, we employed Alizarin Red staining to examine the differentiation of mouse MC3T3-E1 cells. Figure 8d depicts photographic images of Alizarin Red staining 7 and 14 days after culture, and Figure 8e depicts the corresponding quantification of the minerals derived from calcium deposition of MC3T3-E1 cell culture. Both Figure 8d,e indicates that a very significant increase in cell differentiation was observed in the sample with 15% MDHA filler in comparison with the neat PHBV, after both 7 and 14 days of culture. Interestingly, while the unfilled sample had essentially no apparent mineralized nodule on day 7, the PHBV/MDHA composite had substantial differentiation on their surface, demonstrating that DHA particles efficiently stimulate cell differentiation in addition to cell proliferation. These results showed that when 3D DHA particles were combined with PHBV, they significantly increased the cellular activity of preosteoblasts, making them a very promising choice for bone regeneration applications.

4. CONCLUSIONS

In this study, HA particles with a highly regular 3D dandelion geometry were synthesized, and using them, the hypothesis that the use of 3D filler can dramatically improve the physical and mechanical properties of biomedical polymers like PHBV was successfully evaluated. According to the SEM micrographs, the rougher cross section was identified for the DHA-containing composites compared to the controls (neat polymer and NHA composite). A promising and interesting result was based on the examination of the mechanical characteristics,

which demonstrated that the composites incorporated with the DHA and MDHA particles showed significantly higher tensile strength and elastic modulus compared to the neat PHBV and system incorporated with NHA. The significant improvement in mechanical properties for the 3D regular filler (i.e., DHA) compared to the irregular filler (i.e., NHA) supports the hypothesis that the filler geometry has a significant effect on crack prevention and crack deflection to consume fracture energy. In addition to mechanical properties, our research revealed that the as-synthesized 3D DHA filler has a significant impact on the biological properties of biomedical polymers. According to the results, the systems containing DHA and MDHA exhibited a significantly smaller water contact angle compared with the control (i.e., neat PHBV) as a result of the incorporation of HA fillers as hydrophilic particles. While the composite incorporated with DHA and MDHA showed a significantly higher biodegradability in comparison with the neat PHBV, an interesting result was the generation of a dense flake-like apatite layer on the surface of PHBV incorporated with MDHA after 15 days incubation in SBF, confirming the great bioactivity of the PHBV/MDHA composite. According to the findings of this study, the incorporation of the synthesized DHA reinforcing phase at the concentration described in this study has been found to greatly enhance the *in vitro* cellular response to PHBV biomaterials; a significant increase in both the metabolic activity and DNA content of bone cells was detected for the MDHA-filled composites compared to the neat polymer. All of these results imply that mechanical and biological characteristics of biomedical polymers can be controlled by incorporating bioactive fillers having a specific geometry and adjusted surface properties. The approach presented in this study can also provide a fundamental change of view regarding the effect of the characteristics of fillers, including their geometry, on the physical and mechanical properties of biomedical polymers.

AUTHOR INFORMATION

Corresponding Author

Mehdi Sadat-Shojai – Department of Chemistry, College of Sciences, Shiraz University, Shiraz 71454, Iran;
orcid.org/0000-0002-9433-4508; Email: msadatshojai@gmail.com, ms.shojai@shirazu.ac.ir

Authors

Mohammad Kalantari-Lalari – Department of Chemistry, College of Sciences, Shiraz University, Shiraz 71454, Iran
Milad Asadnia – Department of Chemistry, College of Sciences, Shiraz University, Shiraz 71454, Iran

Complete contact information is available at:
<https://pubs.acs.org/10.1021/acsomega.3c05373>

Notes

The authors declare no competing financial interest.

ACKNOWLEDGMENTS

This work was supported by the Shiraz University under grant 98GCB1M256440. We thank Kheng Lim Goh for a useful discussion on the results.

REFERENCES

(1) Alizadeh-Osgouei, M.; Li, Y.; Wen, C. A Comprehensive Review of Biodegradable Synthetic Polymer-Ceramic Composites and their

- Manufacture for Biomedical Applications. *Bioact. Mater.* **2019**, *4*, 22–36.
- (2) Anita Lett, J.; Sagadevan, S.; Fatimah, I.; Hoque, M. E.; Lokanathan, Y.; Léonard, E.; Alshahateh, S. F.; Schirhagl, R.; Oh, W. C. Recent Advances in Natural Polymer-Based Hydroxyapatite Scaffolds: Properties and Applications. *Eur. Polym. J.* **2021**, *148*, 110360.
- (3) Sadat-Shojai, M. Controlled Pattern of Cell Growth in Modulated Protein Nanocomplexes: Regulating Cells Spreading in Three Dimensions. *Mater. Today* **2018**, *21*, 686–688.
- (4) Rong, M.; Zhang, M.; Ruan, W. Surface Modification of Nanoscale Fillers for Improving Properties of Polymer Nanocomposites: A Review. *Mater. Sci. Technol.* **2006**, *22*, 787–796.
- (5) Sadat-Shojai, M.; Khorasani, M. T.; Jamshidi, A.; Irani, S. Nano-Hydroxyapatite Reinforced Polyhydroxybutyrate Composites: A Comprehensive Study on the Structural and In Vitro Biological Properties. *Mater. Sci. Eng., C* **2013**, *33*, 2776–2787.
- (6) Kim, K. H.; Ong, J. L.; Okuno, O. The Effect of Filler Loading and Morphology on the Mechanical Properties of Contemporary Composites. *J. Prosthet. Dent.* **2002**, *87*, 642–649.
- (7) Wang, Y.; Dai, J.; Zhang, Q.; Xiao, Y.; Lang, M. Improved Mechanical Properties of Hydroxyapatite/Poly (ϵ -Caprolactone) Scaffolds by Surface Modification of Hydroxyapatite. *Appl. Surf. Sci.* **2010**, *256*, 6107–6112.
- (8) Liu, Y.; Lu, J.; Cui, Y. Improved Thermal Conductivity of Epoxy Resin by Graphene-Nickel Three-Dimensional Filler. *Carbon Resour. Convers.* **2020**, *3*, 29–35.
- (9) Sadat-Shojai, M.; Khorasani, M. T.; Dinpanah-Khoshdargi, E.; Jamshidi, A. Synthesis Methods for Nanosized Hydroxyapatite with Diverse Structures. *Acta Biomater.* **2013**, *9*, 7591–7621.
- (10) Haider, A.; Haider, S.; Han, S. S.; Kang, I. K. Recent Advances in the Synthesis, Functionalization and Biomedical Applications of Hydroxyapatite: A Review. *RSC Adv.* **2017**, *7*, 7442–7458.
- (11) Sadat-Shojai, M.; Asadnia, M.; Zarei-fard, N.; Arvaneh, A. R. Electrospinning of Liquefied Banana Stem Residue in Conjugation with Hydroxyapatite Nanocrystals: Towards New Scaffolds for Bone Tissue Engineering. *Cellulose* **2022**, *29*, 4039–4056.
- (12) Jirkovec, R.; Holec, P.; Hauzerova, S.; Samkova, A.; Kalous, T.; Chvojka, J. Preparation of a Composite Scaffold from Polycaprolactone and Hydroxyapatite Particles by Means of Alternating Current Electrospinning. *ACS Omega* **2021**, *6*, 9234–9242.
- (13) Sadat-Shojai, M.; Khorasani, M. T.; Jamshidi, A. Hydrothermal Processing of Hydroxyapatite Nanoparticles—A Taguchi Experimental Design Approach. *J. Cryst. Growth* **2012**, *361*, 73–84.
- (14) Yelten-Yilmaz, A.; Yilmaz, S. Wet Chemical Precipitation Synthesis of Hydroxyapatite (HA) Powders. *Ceram. Int.* **2018**, *44*, 9703–9710.
- (15) Yoon, S.; Park, Y.; Park, S.; Stevens, R.; Park, H. Synthesis of Hydroxyapatite Whiskers by Hydrolysis of α -Tricalcium Phosphate Using Microwave Heating. *Mater. Chem. Phys.* **2005**, *91*, 48–53.
- (16) Zhang, H. G.; Zhu, Q. Preparation of Fluoride-Substituted Hydroxyapatite by a Molten Salt Synthesis Route. *J. Mater. Sci.: Mater. Med.* **2006**, *17*, 691–695.
- (17) Baladi, M.; Amiri, M.; Mohammadi, P.; Salih Mahdi, K.; Golshani, Z.; Razavi, R.; Salavati-Niasari, M. Green Sol-Gel Synthesis of Hydroxyapatite Nanoparticles Using Lemon Extract as Capping Agent and Investigation of its Anticancer Activity against Human Cancer Cell Lines (T98, and SHSYS). *Arabian J. Chem.* **2023**, *16*, 104646.
- (18) Reddy, C. S. K.; Ghai, R.; Rashmi; Kalia, V. C. Polyhydroxyalkanoates: An Overview. *Bioresour. Technol.* **2003**, *87*, 137–146.
- (19) Alves, A.; Siqueira, E.; Barros, M.; Silva, P.; Houllou, L. Polyhydroxyalkanoates: A Review of Microbial Production and Technology Application. *Int. J. Environ. Sci. Technol.* **2023**, *20*, 3409–3420.
- (20) Arvaneh, A.-R.; Sadat-Shojai, M. Biodegradable Aliphatic Polyesters for Application in Tissue Engineering. *Iran. J. Polym. Sci. Technol.* **2021**, *34*, 319–348.
- (21) Choi, J.; Lee, S. Y. Process Analysis and Economic Evaluation for Poly (3-Hydroxybutyrate) Production by Fermentation. *Bioprocess Eng.* **1997**, *17*, 335–342.
- (22) Keshavarz, T.; Roy, I. Polyhydroxyalkanoates: Bioplastics with a Green Agenda. *Curr. Opin. Microbiol.* **2010**, *13*, 321–326.
- (23) Sadat-Shojai, M. Calcium Phosphate Reinforced Polyester Nanocomposites for Bone Regeneration Applications. In *Biodegradable Polymeric Nanocomposites: Advances in Biomedical Applications*; Depan, D., Ed., 1st ed.; CRC Press: USA, 2015; pp 1–34.
- (24) Öner, M.; İlhan, B. Fabrication of Poly (3-Hydroxybutyrate-Co-3-Hydroxyvalerate) Biocomposites with Reinforcement by Hydroxyapatite Using Extrusion Processing. *Mater. Sci. Eng., C* **2016**, *65*, 19–26.
- (25) Degli Esposti, M.; Changizi, M.; Salvatori, R.; Chiarini, L.; Cannillo, V.; Morselli, D.; Fabbri, P. Comparative Study on Bioactive Filler/Biopolymer Scaffolds for Potential Application in Supporting Bone Tissue Regeneration. *ACS Appl. Polym. Mater.* **2022**, *4*, 4306–4318.
- (26) Sadat-Shojai, M.; Moghaddas, H. How Geometry, Size, and Surface Properties of Tailor-made Particles Control the Efficiency of Poly (3-hydroxybutyrate-co-3-hydroxyvalerate)/Hydroxyapatite Nanocomposites. *J. Appl. Polym. Sci.* **2020**, *137*, 49810.
- (27) Sadat-Shojai, M.; Moghaddas, H. Modulated Composite Nanofibers with Enhanced Structural Stability for Promotion of Hard Tissue Healing. *Iran. J. Sci. Technol., Trans. A: Sci.* **2021**, *45*, 529–537.
- (28) Sadat-Shojai, M. Electrospun Polyhydroxybutyrate/Hydroxyapatite Nanohybrids: Microstructure and Bone Cell Response. *J. Mater. Sci. Technol.* **2016**, *32*, 1013–1020.
- (29) Monreal Romero, H. A.; Mora Ruacho, J.; Martínez Pérez, C. A.; García Casillas, P. E. Synthesis of Hydroxyapatite Nanoparticles in Presence of a Linear Polysaccharide. *J. Mater.* **2013**, *2013*, 1–5.
- (30) Kokubo, T.; Takadama, H. How Useful is SBF in Predicting In Vivo Bone Bioactivity? *Biomaterials* **2006**, *27*, 2907–2915.
- (31) Ku, K. L.; Grøndahl, L.; Dao, H.; Du, K.; Puttick, S.; Lai, P. L.; Peng, H.; Chu, I. M.; Whittaker, A. K. In Vitro Degradation Study of Polyanhydride Copolymers/Surface Grafted Hydroxyapatite Composites for Bone Tissue Application. *Polym. Degrad. Stab.* **2017**, *140*, 136–146.
- (32) Lee, S. C.; Choi, H. W.; Lee, H. J.; Kim, K. J.; Chang, J. H.; Kim, S. Y.; Choi, J.; Oh, K.-S.; Jeong, Y. K. In-Situ Synthesis of Reactive Hydroxyapatite Nano-Crystals for a Novel Approach of Surface Grafting Polymerization. *J. Mater. Chem.* **2007**, *17*, 174–180.
- (33) Lee, H. J.; Choi, H. W.; Kim, K. J.; Lee, S. C. Modification of Hydroxyapatite Nanosurfaces for Enhanced Colloidal Stability and Improved Interfacial Adhesion in Nanocomposites. *Chem. Mater.* **2006**, *18*, 5111–5118.
- (34) Sadat-Shojai, M.; Ghadiri-Ghalenazeri, S. A Modular Strategy for Fabrication of Responsive Nanocomposites Using Functionalized Oligocaprolactones and Hydroxyapatite Nanoparticles. *New J. Chem.* **2020**, *44*, 20155–20166.
- (35) Al-Saleh, M. H.; Sundararaj, U. Review of the Mechanical Properties of Carbon Nanofiber/Polymer Composites. *Composites, Part A* **2011**, *42*, 2126–2142.
- (36) Šupová, M. Problem of Hydroxyapatite Dispersion in Polymer Matrices: A Review. *J. Mater. Sci.: Mater. Med.* **2009**, *20*, 1201–1213.
- (37) Jia, S.; Yu, D.; Zhu, Y.; Wang, Z.; Chen, L.; Fu, L. Morphology, Crystallization and Thermal Behaviors of PLA-Based Composites: Wonderful Effects of Hybrid GO/PEG via Dynamic Impregnating. *Polymers* **2017**, *9*, 528.
- (38) Zhao, S.; Schadler, L. S.; Duncan, R.; Hillborg, H.; Auletta, T. Mechanisms Leading to Improved Mechanical Performance in Nanoscale Alumina Filled Epoxy. *Compos. Sci. Technol.* **2008**, *68*, 2965–2975.
- (39) Wang, J.; Wu, Y.; Cao, Y.; Li, G.; Liao, Y. Influence of Surface Roughness on Contact Angle Hysteresis and Spreading Work. *Colloid Polym. Sci.* **2020**, *298*, 1107–1112.

(40) Lyu, S.; Untereker, D. Degradability of Polymers for Implantable Biomedical Devices. *Int. J. Mol. Sci.* **2009**, *10*, 4033–4065.

(41) Liang, H.; Wang, Y.; Chen, S.; Liu, Y.; Liu, Z.; Bai, J. Nano-Hydroxyapatite Bone Scaffolds with Different Porous Structures Processed by Digital Light Processing 3D Printing. *Int. J. Bioprint.* **1970**, *8*, 502.